Available online at www.sciencedirect.com
SCIENCE DIRECT
Neuropharmacology 50 (2006) 512–520
NEURO PHARMACOLOGY
www.elsevier.com/locate/neuropharm

Characterisation and differential expression of two very closely related G-protein-coupled receptors, GPR139 and GPR142, in mouse tissue and during mouse development

Ute Süsens, Irm Hermans-Borgmeyer, Jens Urny, H. Chica Schaller*

Zentrum für Molekulare Neurobiologie, Universität Hamburg, Martinistr. 52, D-20246 Hamburg, Germany

Received 27 July 2005; received in revised form 31 October 2005; accepted 2 November 2005

Abstract

By searching the human and mouse genomic databases we found two G-protein-coupled receptors, GPR139 and GPR142, with characteristic motifs of the rhodopsin family of receptors. The gene for GPR139 maps to chromosome 7F1 of mouse and 16p12.3 of human and that for GPR142 to 11E2 of mouse and 17q25.1 of human. We isolated GPR139 from a cDNA library of adult mouse brain and GPR142 from a cDNA library of brains from 15-day-old mouse embryos. GPR139 mRNA was predominantly expressed in specific areas of human and mouse brains, whereas GPR142 mRNA showed a more ubiquitous expression both in the brain and in various peripheral glands and organs. A 50% identity and a 67% homology at the amino-acid level between the two receptors and only 20–25% identity with other G-protein-coupled receptors established them as a new subbranch within the phylogenetic tree and hints at a common or similar ligand(s). Preliminary results suggest that the cognate ligand is present in brain extracts and is, most likely, a small peptide. GPR139 signal transduction in Chinese hamster ovary cells requires coupling to an inhibitory G-protein and is mediated by phospholipase C. Dimer formation may be necessary for proper function.
© 2005 Elsevier Ltd. All rights reserved.

Keywords: G-protein-coupled receptor; GPR139; GPR142; Mouse-brain expression; Signal transduction; Dimerisation

1. Introduction

G-protein-coupled receptors (GPCRs) are the largest family of cell-surface receptors transducing signals from the extracellular environment to intracellular effectors. Ligands are of diverse molecular structure and size and include light, ions, amino acids, nucleotides, metabolic intermediates, lipids, peptides and proteins (Civelli, 2005). GPCRs are characterised by seven transmembrane helices separated by intra- and extracellular loops of variable lengths. Together with the extracellular amino terminus and the cytosolic carboxy terminus the loops determine ligand interactions and signal-transduction pathways (Bockaert and Pin, 1999). The classification of GPCRs into subfamilies is based on their homology within the heptahelical structure and partially on their interaction with ligands (Frederiksson et al., 2003a). GPCRs play key physiological roles, both during development and in the adult, and their dysfunction is implicated in several diseases (Hökfelt et al., 2003). This is reflected by the fact that about half of the current drugs, and certainly more in the future, are targeted to GPCRs. Discovery of novel receptors and their ligands is, therefore, of great interest for pharmacology.

In this paper we describe the identification, cloning and tissue distribution of two mouse GPCRs, GPR139 and GPR142, which belong to the rhodopsin family of GPCRs. They are highly related to each other, but differ strongly in expression

* Corresponding author. Tel.: +49 40 42803 6277; fax: +49 40 42803 5101.
E-mail address: schaller@zmnh.uni-hamburg.de (H.C. Schaller).

0028-3908/$ - see front matter © 2005 Elsevier Ltd. All rights reserved.
doi:10.1016/j.neuropharm.2005.11.003

patterns within the brain and in other tissues. A ligand present in brain extracts activated Ca^{2+} mobilisation in GPR139-expressing cells. Signalling was mediated by an inhibitory G-protein and by phospholipase C and required dimer formation for proper function.

2. Materials and methods

2.1. Identification and cloning of mouse GPR139 and GPR142

By searching the human genomic database with known peptide GPCRs using TBLASTN we discovered GPR139 and GPR142. The conserved regions of the human receptors subsequently served to find the respective mouse orthologues. A full-length cDNA for mouse GPR139 was obtained by 5′- and 3′-rapid amplification of cDNA ends (RACE) from a RACE-ready cDNA of mouse brain (Ambion, Huntingdon, UK). Nested RACE primers were designed over an internal XbaI site at position 300 of the mouse nucleotide sequence (AY485344), which allowed amplification of a 1600-bp 3′-fragment and a 420-bp 5′-fragment containing start and stop codons, respectively, and covering an open-reading frame of 345 amino acids. The sequence around the stop codon was present in two ESTs (CF727486 and BU610327), and one EST from a CAP-trapped cDNA of embryonal day (E) 11 spinal cord (BB870915) covered start and first splice site of GPR139 confirming correctness of our mouse cDNA sequence. The resulting PCR fragments were digested with XbaI, ligated and cloned into the pGEM-T-easy vector (Promega, Heidelberg, Germany). The full-length open-reading frame, provided with EcoRI and XhoI at the start and stop sites, respectively, was then introduced into pcDNA5/FRT and pcDNA5/FRT/TO (Invitrogen, Karlsruhe, Germany), which contained sequences coding for a signal peptide and a hemagglutinin (HA) tag in front of the EcoRI site (Ignatov et al., 2003a).

A similar approach was attempted to clone GPR142. Various cDNA libraries were probed by 5′ and 3′ RACE with nested primers over an internal BsrFI site at position 600 of the mouse nucleotide sequence (AY957501), but did not yield the expected fragments. In the end, primers close to predicted stop and several possible start codons and conserved internal sites were designed and used to amplify cDNA fragments from a home-made cDNA library of E15 mouse brain. After fragment annealing a full-length clone was obtained, which coded for a protein of 371 amino acids. Since GPR142 contained an internal EcoRI site, it was provided with a HindIII site at the start and an XhoI site after the stop position before insertion into appropriate mammalian expression vectors. All constructs were verified by sequencing. The full-length sequences of mouse GPR139 and GPR142 were submitted to GenBank under the accession numbers AY485344 and AY957501, respectively.

2.2. Tissue distribution

A mouse multiple-tissue and a mouse-embryo northern blot and the human-brain blots II and IV (all from Clontech, Heidelberg, Germany) were hybridised with [α^{32}P]-dATP-labeled probes covering nucleotides 92–1035 and 295–1035 of mouse GPR139 and nucleotides 571–1012 of mouse GPR142.

A mouse multiple-tissue cDNA panel (Clontech) was used as template for PCR with nested primers for GPR139 from nucleotides 157–180 and 291–310 and for GPR142 from nucleotides 571–594 and 599–623, each amplified against a primer close to the stop codon, namely 1012–1035 for GPR139 and 1086–1113 for GPR142. Amplification of glyceraldehyde-3-phosphate dehydrogenase (GAPDH) served as control.

For in situ analysis antisense and sense probes corresponding to nucleotides 294–1035 of GPR139 and 571–1113 of GPR142 were labeled with [α^{35}S]-UTP and used on cryosections from adult mouse brain and mouse embryos, essentially as described earlier (Süsens et al., 1997).

2.3. Aequorin-based Ca^{2+}-bioluminescence and luciferase-reporter-gene assays

GPR139 and GPR142 plasmids were stably integrated into CHO-K1 and for inducible expression into HEK-293 cells using the appropriate flip-in systems (Invitrogen). Clones were selected by treating cells with 500 μg/ml and 100 μg/ml of hygromycin. Stable expression was monitored by western blotting and cell-surface expression by FACS with the monoclonal antibody HA.11 (Eurogentec, Köln, Germany), which recognises the amino-terminal HA tag. For Ca^{2+} analysis stable GPR139 and GPR142 cell lines were transiently transfected by electroporation with vectors containing the mitochondrially targeted Ca^{2+} sensor apoaequorin, CIN/mtAEQ, and the promiscuous G-protein subunit, Gα16, pCIH/G16, both kindly provided by Stables et al. (1997). Likewise, reporter-gene constructs containing cAMP-, serum-, and multiple-response elements in front of the luciferase gene (Fitzgerald et al., 1999; Jiang et al., 2003) were introduced into the stable GPR139- and GPR142-expressing cell lines by electroporation. As control served the flip-in CHO-K1 cell line, stably expressing human SALPR (UMR cDNA Resource Center, Rolla, USA), integrated like GPR139 and GPR142 with signal peptide and HA tag into the pcDNS5/FRT vector (Boels et al., 2004). Twenty-four hours after transfection serum-containing medium was replaced with serum-free defined medium, as described earlier (Ignatov et al., 2003a). To measure the Ca^{2+}-induced luminescence cells were treated at room temperature for 4 h with 2.5 μM coelenterazine (Invitrogen) as cofactor for aequorin. Ligands were dissolved in serum-free medium, added to the cells and the luminescence was measured for 15 s in a luminometer (PerkinElmer, Rodgau, Germany). For the reporter-gene assay cells were incubated for 5 h at 37 °C with increasing concentrations of ligands and, after incubation for 2 min in Bright-Glo (Promega), the luminescence was measured for 1 s in a luminometer.

2.4. Peptides, peptide-enriched extracts and inhibitors

Peptides were purchased from Bachem (Weil am Rhein, Germany), Sigma–Aldrich (Taufkirchen, Germany) and Phoenix Europe (Karlsruhe, Germany). Porcine brain acetone powder (Sigma–Aldrich) was extracted with methanol and purified over C18-Seppak as described earlier (Kayser et al., 1998). Cells were pretreated overnight with 4 nM of the proteasome inhibitor MG-132 (Calbiochem, Bad Soden, Germany), for 4 h with 200 ng/ml pertussis toxin (Sigma–Aldrich) and for 10 min with 5 μM U73122 (Merck, Darmstadt, Germany).

3. Results

3.1. Identification, cloning and structure of mouse GPR139 and GPR142

The human genomic database was searched for novel sequences related to peptide-binding GPCRs using TBLASTN. Two related sequences were found in the human genome, one located on chromosome 16p12.3 and the other on 17q25.1. They shared 50% amino-acid identity in a region behind a splice site within the first transmembrane region. With their help mouse orthologues were also discovered, located on chromosomes 7F1 and 11E2. While this work was in progress human and mouse sequences were predicted and designated GPR142 and GPR139 (Frederiksson et al., 2003b; Gloriam et al., 2005), names which for simplicity sake (Foord et al., 2005) we adopted. Predictions for the amino-terminal domain and the start codons were complicated by the presence of various splice possibilities in the human and mouse genomes. We therefore designed nested primers in the conserved parts to identify mouse cDNAs by 5′- and 3′-RACE. GPR139 was amplified from adult and GPR142 from E15 mouse brain. The full-length clones coded for 345 and 371 amino acids, respectively, were submitted to GenBank

(accession numbers AY485344 for GPR139 and AY957501 for GPR142). The mouse sequence for GPR139 is identical to one recently published as GPRg1 (Matsuo et al., 2005).

An alignment between GPR139 and GPR142 of mouse shows 50% amino-acid identity (Fig. 1) and 67% homology. GPR139 is encoded by two exons, both in mouse and human, whereas GPR142 consists of three exons in mouse, and three (Matsuo et al., 2005) or four (Frederiksson et al., 2003b) are predicted for human. The splice sites between exons one and two of GPR139 and exons two and three of GPR142 are located at an identical position in the first transmembrane domain, indicated by an open triangle in Fig. 1. After the splice site the sequence of both receptors contains a conserved asparagine, which is typical for many GPCRs. This asparagine is part of a six-amino-acid deletion predicted, probably wrongly, for the mouse GPR139 sequence (Gloriam et al., 2005). Other highly conserved residues and motifs common for GPCRs of the rhodopsin family (Bockaert and Pin, 1999) are highlighted in Fig. 1. Both receptors contain a single N-glycosylation site in the extracellular amino-terminal domain, but lack cysteines in extracellular loops one and two, a hallmark for GPCRs necessary for disulfide bonding.

For other receptors a thorough phylogenetic analysis had helped to predict possible ligands (Joost and Methner, 2002; Ignatov et al., 2003a,b). The high identity of 50% between

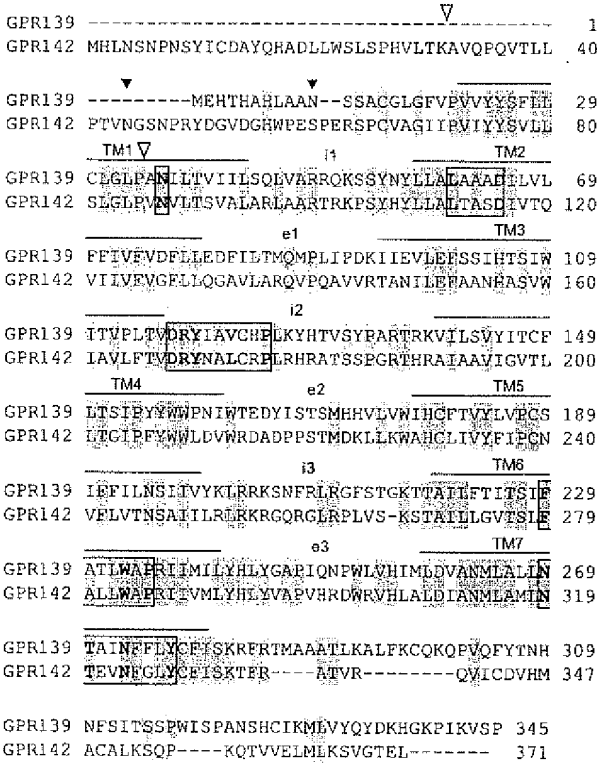

Fig. 1. Comparison of amino-acid sequence and structure of mouse GPR139 and GPR142. Identical amino acids are shaded in grey. The seven putative transmembrane domains (TM1–TM7) are overlined and the intra- and extracellular loops indicated by i1–i3 and e1–e3, respectively. Motifs typical for the rhodopsin family of GPCRs are encased and the characteristic amino acids highlighted in italics. N-glycosylation sites are marked by filled and splice sites by open triangles.

Table 1
Phylogenetic analysis of mouse GPR139 and GPR142

	GPCR	Identity (%)	Similarity (%)	*E*-value
GPR139	GPR142	50	67	1e−76
	TRH-R	22	41	4e−14
	DOR-1	21	44	5e−14
	SS4R	22	45	5e−14
	CCR-1	23	45	3e−13
	KOR-3	22	45	4e−13
GPR142	GPR139	50	67	1e−76
	SS4R	25	41	8e−11

The full-length amino-acid sequences of mouse GPR139 and GPR142 were used to analyse the phylogenetic relationship with other mouse GPCRs. For GPR139 the six first BLAST hits are given, for GPR142 only two (due to the very low *E*-values).

mouse GPR139 and GPR142 is suggestive of a common or similar ligand(s). Their relatedness to other members of the rhodopsin family of GPCRs was not very revealing and included peptide and chemokine receptors with identities in the range of 20–25% (Table 1).

3.2. Tissue distribution of mouse GPR139 and GPR142

To study expression an adult multiple-tissue and an embryo northern blot of mouse were hybridised with a probe covering nucleotides 92–1035 of GPR139. GPR139, as message of around 5.5 kb, was exclusively expressed in the brain and was present strongly in E15 and E17 and very weakly in E11 embryos (Fig. 2A). Two human brain-specific northern blots were assayed with a probe covering nucleotides 295–1035 of mouse GPR139 and showed predominant expression in putamen, medulla and caudate nucleus. Weaker signals were present in thalamus, amygdala, and spinal cord. In addition to the 5.5-kb band a smaller band of around 3.5 kb was present suggesting differential splicing (Fig. 2B). The same northern filters were hybridised with a probe covering nucleotides 571–1012 of mouse GPR142. No distinct signal, but only a broad smear with varying levels of intensity in the different tissues was obtained. Strongest signals were present in E15 mouse embryos and in various regions of the human brain including cerebral cortex, cerebellum and spinal cord (data not shown). The smear is indicative of fast mRNA turnover and degradation and may explain the absence of GPR142 ESTs in the mouse and human databases.

To confirm the tissue distribution of GPR139 and GPR142, a mouse multiple-tissue cDNA panel was probed with the nested primers designed for the 3′-RACE around position 300 of GPR139 and 600 of GPR142 of the nucleotide sequence and amplified against a primer close to the respective stop codons. Fragments of the expected sizes of 794 bp for GPR139 and 444 bp for GPR142 were obtained (Fig. 2C). GPR139 was most prominently expressed in the brain and in E11, E15 and E17 mouse embryos, and a weak signal was present in mouse testis. These results are in agreement with the data obtained by northern-blot analysis and with ESTs, which documented presence of GPR139 in E12.5–E14.5 eyes, E11 spinal cord

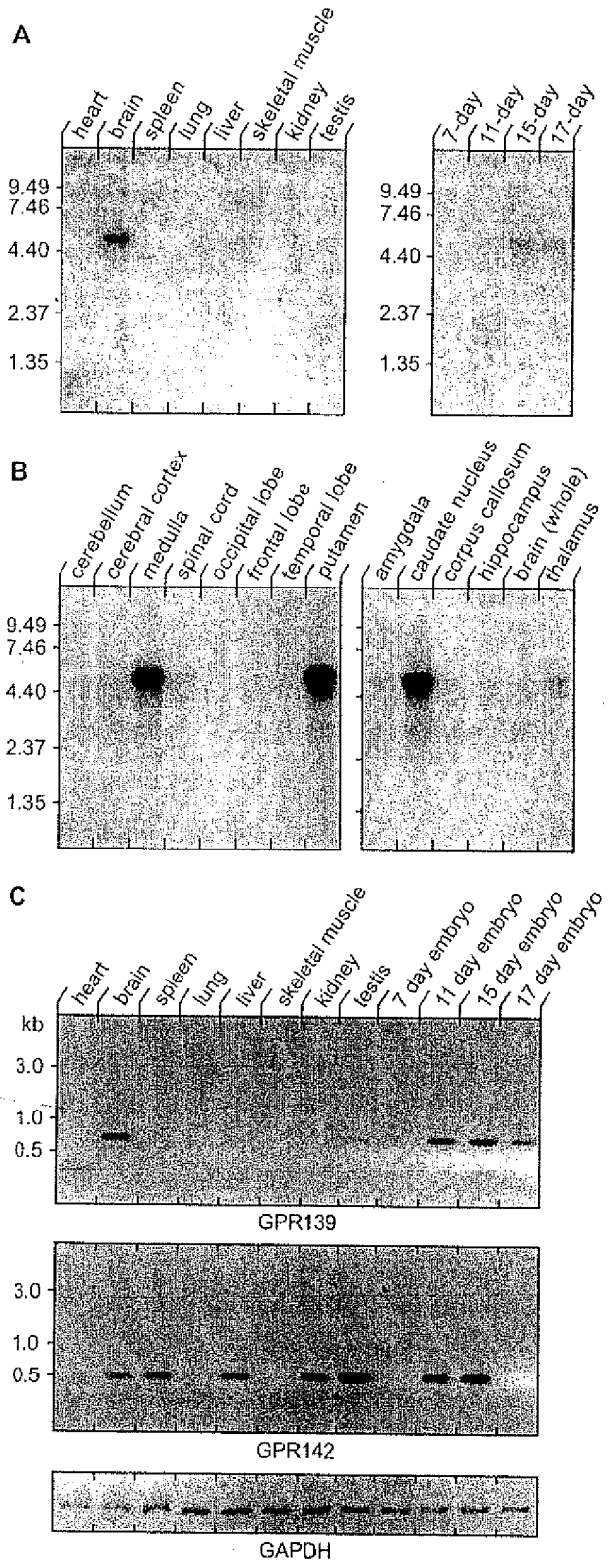

Fig. 2. GPR139 mRNA expression in different mouse tissues and in human brain. (A) An adult mouse multiple-tissue and a mouse-embryo northern blot were hybridised with a radiolabeled probe (nucleotides 92–1035) covering most of the open-reading frame of mouse GPR139. (B) Two human brain northern blots were probed with a shorter fragment representing the amino-terminal second exon (nucleotides 295–1035) of mouse GPR139. (C) GPR139 and GPR142 mRNA expressions were analysed by PCR using a cDNA panel prepared from adult mouse tissues and whole embryos. Gene-specific nested primers were used to amplify a 745-bp fragment of GPR139 (upper panel) and a 444-bp fragment of GPR142 (middle panel). GAPDH amplification served as control (lower panel).

and adult mouse brain. Strong expression of GPR142 was found in the testis, E11 and E15 embryos, kidney and spleen. Weaker GPR142 expression was evident in brain and liver.

3.3. Differential expression of GPR139 and GPR142 in the adult and developing mouse brain

To analyse the expression pattern of GPR139 and GPR142 in the brain in more detail, we performed in situ hybridisations using [α^{35}S]-labeled riboprobes. Sense and antisense probes covered nucleotides 294–1035 of GPR139 and 571–1113 of GPR142. In the adult mouse brain intense hybridisation signals of GPR139 were restricted to the median habenular nucleus (Fig. 3A, B), while transcripts of GPR142 were observed in all the areas of brain with an intense labeling of the hippocampus and the dentate gyrus and weaker signals in the median habenula (Fig. 3C, D).

In situ hybridisation analysis on sagittal sections through murine embryos at E12.5 and E18.5 showed that GPR139 transcripts were detected exclusively in distinct regions of the brain and in spinal cord with slightly increasing intensities towards E18.5 (Fig. 4A, B). In contrast, GPR142 expression was observed primarily outside the central nervous system in a ubiquitous manner with highest labeling seen over thymus, liver and cartilage (Fig. 4A', B'). Coronal sections through mouse heads at E18.5 demonstrated that indeed GPR139 transcripts were present only in restricted regions of the CNS, while those of GPR142 were observed in all areas of the developing brain with a few areas exhibiting more intense hybridisation signals (Fig. 5). GPR139 transcripts accumulated in the CA1 area of the hippocampus and over the median habenular nucleus (Fig. 5D, E), and signals of lower intensity were detected over the lateral habenular nucleus (Fig. 5E). In the midbrain area the nucleus oculomotoris (Fig. 6F) and in the hindbrain the nucleus hypoglossis (Fig. 5L) were highlighted by signals. Lower intensities were detected over the piriform and enterorhinal cortices (Fig. 5B, F), the lateral septum (Fig. 5B), the amygdala (Fig. 5C), a few median thalamic nuclei, the reticular nucleus of the thalamus (Fig. 5C, D), the central gray (Fig. 5G), the inferior colliculus (Fig. 5G–I), the medial vestibular nucleus and the inferior olive (Fig. 5I, J). As mentioned above GPR142 expression was observed in neuronal and non-neuronal cell populations of the head with lower hybridisation intensities over the fiber tracts. Brain areas highlighted by more intense hybridisation signals included the cerebral cortex (Fig. 5A'–F'), the median thalamic nuclei

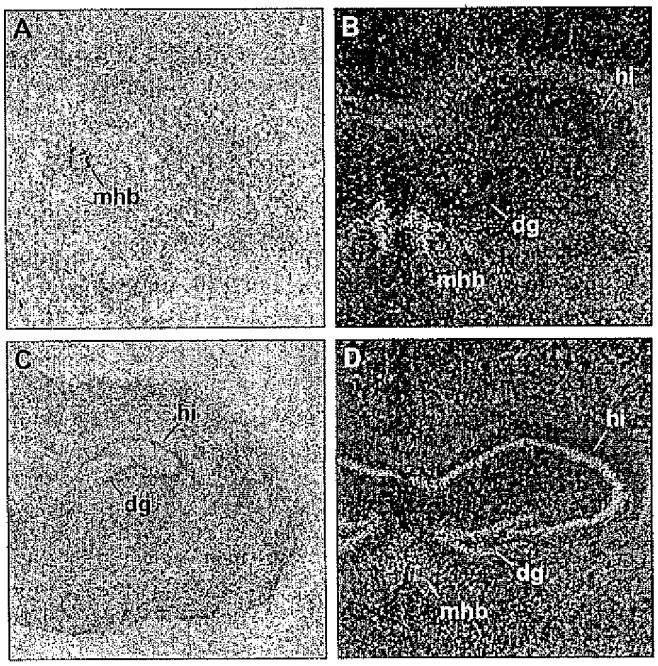

Fig. 3. Distribution of GPR139 and GPR142 transcripts in the adult mouse brain. Coronal sections through an adult mouse brain were prepared at the level of the hippocampus and hybridised to [α^{35}S]-UTP-labeled riboprobes specific for GPR139 (A, B) and GPR142 (C, D). (B, D) Higher magnifications of the hippocampal area are shown as photomicrographs under darkfield illumination of emulsion-dipped coronal sections. Dg, dentate gyrus; hi, hippocampus; and mhb, median habenular nucleus.

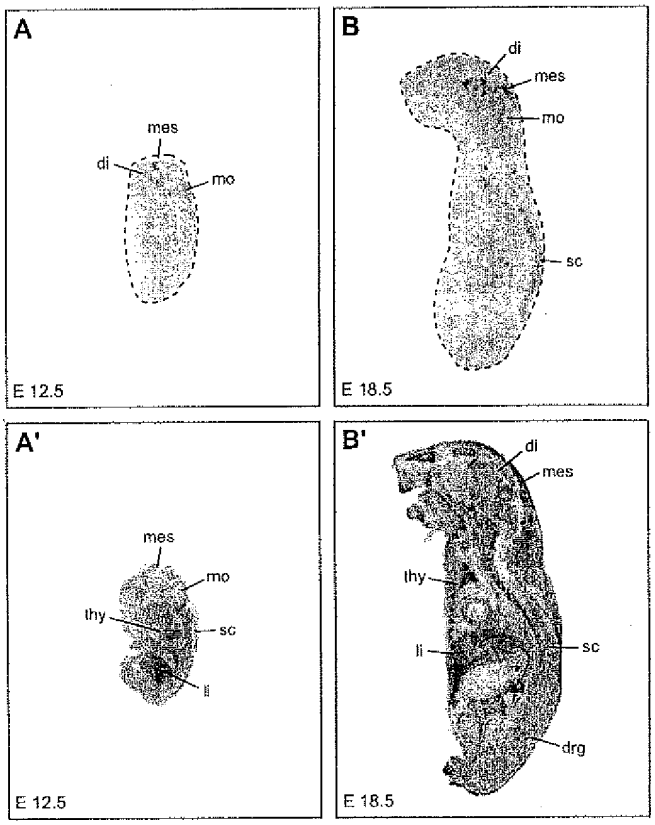

Fig. 4. GPR139 and GPR142 expressions during embryonic development. Sagittal sections through mouse embryos at E12.5 (A, A') and E18.5 (B, B') were hybridised to sense probes specific for GPR139 (A, B) and GPR142 (A', B'). In the presented autoradiograms the ventral surface is to the left. Di, diencephalons; drg, dorsal-root ganglion; li, liver; mes, mesencephalon; mo, medulla oblongata; sc, spinal cord; and thy, thymus.

(Fig. 5C', D'), the anterior hypothalamic nucleus (Fig. 5C'), the CA3 region of the hippocampus (Fig. 5C'–E'), the facial nucleus (Fig. 5H') and the inferior olive (Fig. 5I'–K'). In contrast to GPR139 GPR142 transcripts were also observed in the neuronal and non-neuronal parts of the retina (Fig. 5A'), and transcripts were present in the peripheral nervous system. The sensory epithelia of the cochlea (Fig. 5F'–H') expressed GPR142 as did the lateral portion of the trigeminal ganglion (Fig. 5C', D', shown at higher magnification in Fig. 5N, N'). The sense probes served as controls and did not elicit specific responses.

3.4. Heterologous expression, ligand screening and signal transduction

For heterologous expression GPR139, GPR142 and SALPR (as control) were inserted into mammalian vectors, which provided a signal-peptide sequence to improve cell-surface expression and a hemagglutinin tag to monitor trafficking. Transient expression resulted in low transfection efficiencies for both receptors in all cell lines assayed. We assume that the missing S–S bridge between extracellular loops one and two is responsible for destabilisation of the protein structure, especially when protein folding is under stress due to overexpression. Stable expression was established in the flip-in cell lines CHO-K1 and HEK-293, the latter under an inducible promoter. No endogenous expression of GPR139 and of GPR142 was found by northern and RT-PCR analyses. In both stable cell lines GPR139 was more strongly expressed than that of GPR142, as shown for CHO-K1 cells in Fig. 6A–F. This finding was supported by FACS analysis, where cell-surface expression of GPR139 was in the range of 70–80% compared to only 15–25% of GPR142. Expression of GPR142 and cell-surface trafficking could be improved by pretreating cells with the proteasome inhibitor MG-132 (Fig. 6G, left panel). This suggests that misfolding of GPR142 during biosynthesis may hinder the transport from the endoplasmic reticulum to the outer cell membrane. In HEK-293 cells GPR139 appeared as monomer and in CHO-K1 cells as dimer (Fig. 6G, middle panel). PNGase treatment resulted in only a slight shift to a single band of a molecular mass still in the dimer range (Fig. 6, right panel). This indicates that a partner or conditions are present in CHO-K1, but not in HEK-293 cells, which favour dimer formation and potential functions.

To analyse possible ligands we concentrated on GPR139 because of its higher protein-expression levels and better presentation at the outer cell membrane. As most sensitive method to screen for ligands we preferentially used the Ca^{2+}-mobilisation assay. For that purpose CHO-K1 cells, stably expressing the receptor under investigation, were transiently transfected with apoaequorin which, together with its

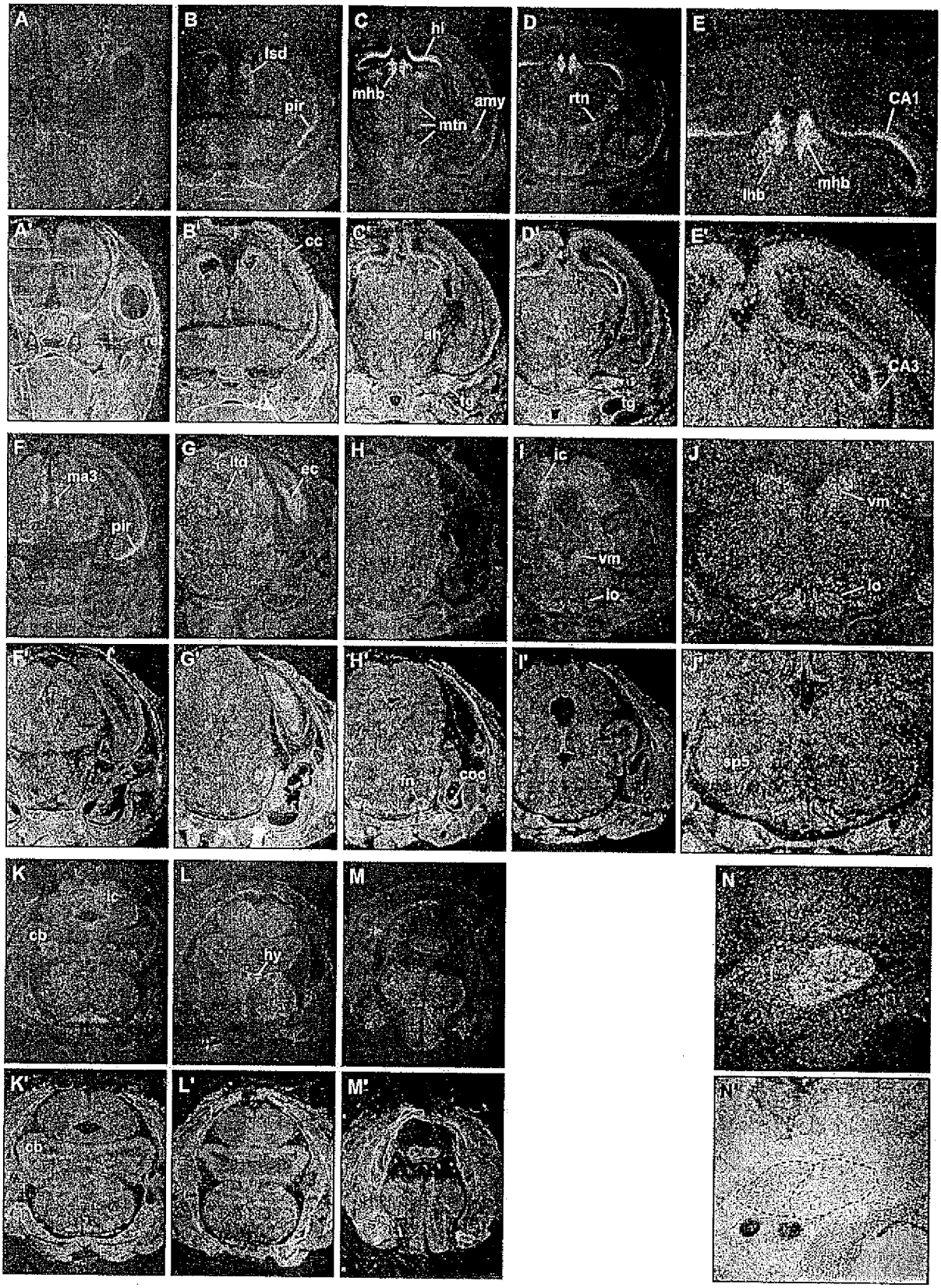

Fig. 5. Expression of GPR139 and GPR142 in the embryonic mouse brain. Darkfield photomicrographs of emulsion-dipped coronal sections of a mouse head at E18.5, hybridised to the GPR139 (A–M) and GPR142 (A'–N', N) sense probes, are shown in rostral to caudal direction. (E) and (E') are higher magnifications of the hippocampal area in (D) and (D'), and (N) and (N') of (D') highlighting expression of GPR142 in the trigeminal ganglion. Ah, anterior hypothalamic nucleus; amy, amygdala; CA1, CA1 region of the hippocampus; CA3, CA3 region of the hippocampus; cb, cerebellum; cc, cerebral cortex; coc, cochlea; ec, enterorhinal cortex; fn, facial nucleus; hi, hippocampus; hy, nucleus hypoglossis; ic, inferior colliculus; io, inferior olive; lhb, lateral habenular nucleus; lsd, lateral septum; ltd, laterodorsal tegmental nucleus; ma3, medial accessory oculomotor nucleus; mhb, median habenular nucleus; mtn, median thalamic nuclei; pir, piriform cortex; ret, retina; rtn, reticular nucleus of the thalamus; sp5, spinal trigeminal nucleus; t, tongue; tg, trigeminal ganglion; tn, median thalamic nuclei; and vm, ventral vestibular nucleus.

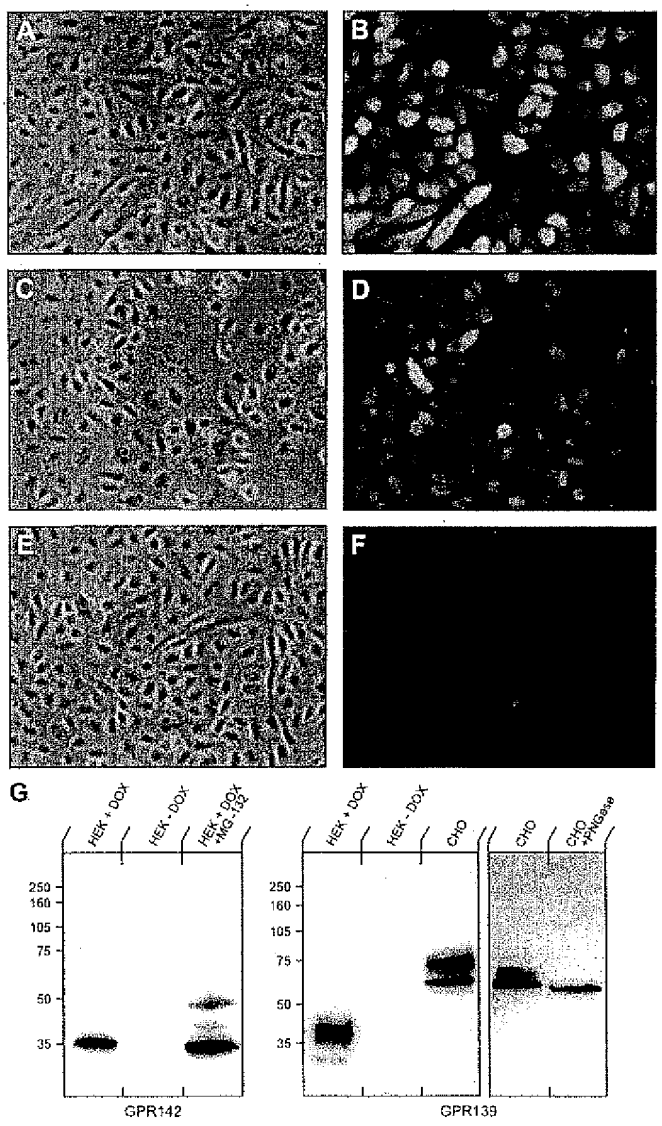

Fig. 6. Stable expression of GPR139 and GPR142 in CHO-K1 and HEK-293 cells. (A–F) Protein expression of GPR139 (A, B, E, and F) and GPR142 (C, D) was visualised with an antibody against the amino-terminally located hemagglutinin tag (A–D). Incubation without first antibody served as control (E, F). Shown in the left are phase-contrast and in the right fluorescent photomicrographs. (G) Stimulation of GPR142 protein expression by the proteasome inhibitor MG-132 and dimer formation of GPR139 in CHO-K1 and not in HEK-293 cells. GPR142 (left panel) and GPR139 (middle panel) expressions were visible in stably transfected HEK-293 cells after induction with doxycycline (DOX). Pretreatment of HEK-293 cells with the proteasome inhibitor MG-132 improved protein stability of GPR142 (left panel, third lane). In CHO-K1 cells GPR139 migrated in a molecular mass range of a dimer (middle panel, third lane). Treatment with PNGase F resulted in reduction to a single band still in the dimer range (right panel, second lane). The immunoblots were visualised with antibodies against the hemagglutinin tag.

cofactor coelenterazine, functions as calcium sensor. Ligands interacting with Gq-coupled GPCRs should give rise to an increase in Ca^{2+}-bioluminescence due to Ca^{2+} release from internal stores. In order to monitor responses to Gs- and Gi-coupled GPCRs, in addition to apoaequorin the promiscuous Gα16 subunit was co-transfected, which also stimulates Ca^{2+} release from internal stores. Without reproducible effects on GPR139 in the Ca^{2+}-mobilisation assay were neuropeptides, such as thyrotrophin-releasing hormone, opioid peptides, somatostatin, cortistatin, nociceptin, neurotensin, gonadotrophin-releasing hormone, urotensin, motilin, secretoneurin, substance P, apelin and CART (cocaine- and amphetamine-regulated transcripts) peptide, chemokines, such as RANTES and fMLP, and steroid hormones, such as estradiol, progesterone and dexamethasone. Peptides and chemokines were applied at nano-to-micromolar, steroid hormones at micromolar concentrations. Neuromedin B and bombesin elicited endogenous responses, both in GPR139- and SALPR-expressing cells. A strong positive effect was achieved reproducibly with an acetone extract from porcine brain, which had been further purified by methanol extraction and reverse-phase chromatography to enrich for small peptides. A stepwise elution from C18-Seppak cartridges yielded an 80% methanol fraction, in which a ligand was enriched that stimulated Ca^{2+} mobilisation tenfold better in GPR139-expressing cells than that in SALPR-expressing cells (Fig. 7). Stimulation with the endogenous ligand ATP (Stables et al., 1997) was used to control the system. Extracts purified from other sources, like pancreas, placenta, serum and diverse cell lines, showed no effects indicating predominant presence of a GPR139-specific ligand in the brain. Signal transduction did not depend on the presence of Gα16 and was inhibited by pretreatment with pertussis toxin and the phospholipase C inhibitor U73122 (Fig. 8A). The inhibitors, at the concentrations used, had no influence on the basal response elicited by medium without added ligands (Fig. 8B).

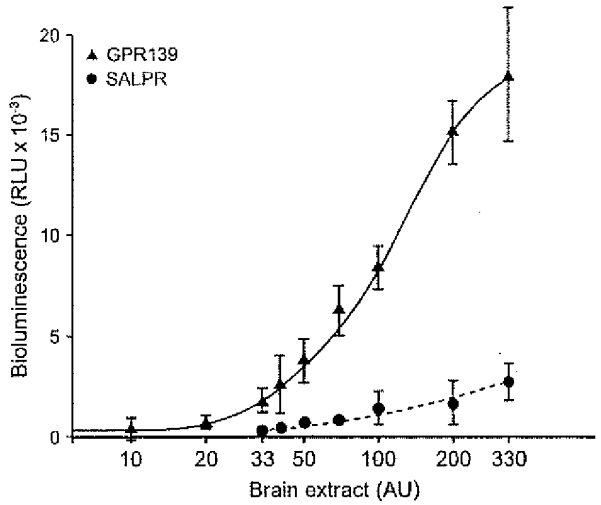

Fig. 7. A ligand present in brain extracts stimulates Ca^{2+} mobilisation in CHO-K1 cells stably expressing GPR139. CHO-K1 cells, stably expressing GPR139 or as control SALPR, were transiently transfected with vectors coding for apoaequorin as Ca^{2+} sensor and with Gα16 to improve signalling. The Ca^{2+}-induced bioluminescence is presented as relative light units (RLU) from which the basal medium response was subtracted. Ca^{2+} mobilisation was dose-dependently increased by incubation in a peptide-enriched extract from porcine brain. The concentration of the brain extract is given in arbitrary units (AU), as calculated from the respective dilutions. The results are averaged over three to six independent measurements for each concentration and are presented as means ± SD.

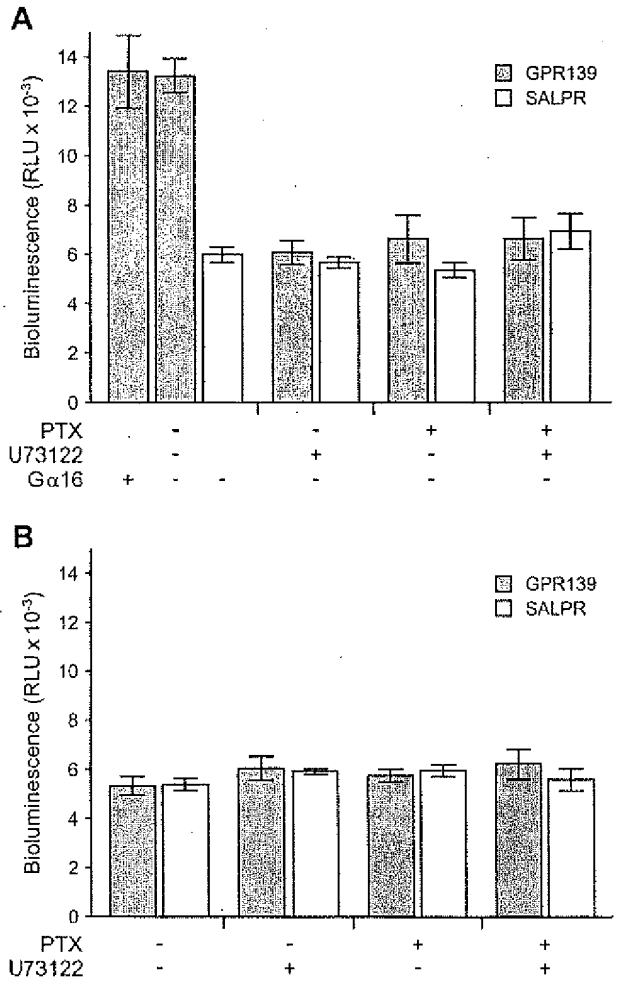

Fig. 8. Analysis of signal transduction in CHO-K1 cells stably expressing GPR139 or SALPR. To monitor Ca^{2+} mobilisation cells were transiently transfected with apoaequorin alone or together with Gα16. Cells were pretreated for 4 h with 200 ng/ml pertussis toxin (PTX) or for 10 min with 5 μM U73122 before the brain extract corresponding to a concentration of 100 arbitrary units of Fig. 7 (A) or medium (B) was added and bioluminescence recorded. The Ca^{2+}-induced bioluminescence is given in relative light units (RLU) and is presented as means ± SD. The data are representative of at least three independent experiments.

Since both pertussis toxin and U73122 inhibited Ca^{2+} mobilisation of the brain extract, a clear distinction between Gi and Gq coupling was not possible. Therefore, the brain extract was also tested in the luciferase-reporter assay. For that purpose CHO-K1 cells stably expressing the receptor were transiently transfected with the luciferase-reporter construct. In combination with forskolin Gi-coupled receptors decrease and Gs- and Gq-coupled receptors increase the luciferase activity. We found that the forskolin-stimulated activation in the luciferase-reporter assay was significantly inhibited by increasing concentrations of the brain extract in GPR139- and much less in SALPR-expressing cells (Fig. 9). Treatment with ATP increased the forskolin response in both cell lines to a similar extent (Fig. 9). We take this as evidence that the effect of the brain extract on GPR139 is predominantly mediated by an inhibitory G-protein.

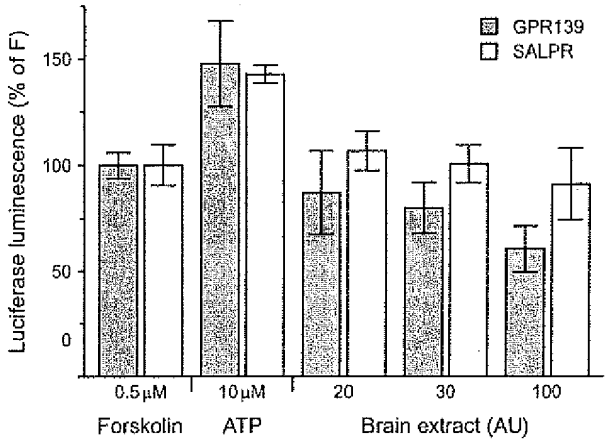

Fig. 9. GPR139 signalling is mediated by an inhibitory G-protein. The forskolin-induced increase in luminescence in the luciferase-reporter assay was inhibited by increasing concentrations of the brain extract and stimulated by ATP. The increase in luciferase activity, achieved by treatment with 0.5 μM forskolin, from which the basal response to medium was subtracted, was defined as 100%. Effects are expressed as percentage of the forskolin stimulation (% of *F*) and given as means ± SD. The experiment was repeated at least three times.

4. Discussion

The mouse G-protein-coupled receptors GPR139 and GPR142 show with 94% and 74% identity at the amino-acid level, respectively, a high degree of relatedness to their human counterparts, which suggests a conserved function in evolution. The two receptors in mouse share 50% of their amino acids with each other, suggestive of a common ligand. The relatedness of 20–25% to other members of the rhodopsin family included receptors for thyrotrophin-releasing hormone, opioid peptides, somatostatin, nociceptin and chemokines, which did not allow precise prediction of possible ligands or the ligand class. We tested the respective and several other peptides, chemokines and steroids in various ligand-receptor assays, but none proved positive. A stimulating effect, both in GPR139-expressing cells and in controls, was obtained with neuromedin B and the related peptide bombesin and categorised as endogenous. As control we used cell lines transfected with an identical vector construct coding for a similar GPCR and selected with the same antibiotics. We chose SALPR because its cell-surface expression was similar to that of GPR139. A reproducible, dose-dependent and specific response was obtained with a peptide-enriched brain extract. Signal transduction induced by the brain extract was inhibited by pertussis toxin indicating coupling of GPR139 to an inhibitory G-protein. Signalling was also blocked by the phospholipase C inhibitor U73122, which normally indicates coupling to Gq. In line with this we found that the endogenous ATP response, which is mediated by a Gq-coupled ATP receptor, was not influenced by pertussis toxin, but completely abolished by U73122. Phospholipase C is also activated by βγ subunits of G-proteins. We therefore assume that interaction of the brain extract with GPR139 activated phospholipase C via the release of βγ subunits. The neuromedin B response was inhibited by U73122 and not

by pertussis toxin confirming the notion that it is not the ligand present in brain extracts.

A strange finding was that GPR139 and GPR142 are present in HEK-293 cells as monomers, whereas in CHO-K1 cells GPR139 only exists as dimer. The hemagglutinin tag at the amino terminus allowed cell-surface detection and revealed presence of both forms at the outer cell membrane. The response of the brain extract on GPR139 was only observed in CHO-K1 cells and not in HEK-293 cells. This could mean that a partner is present in CHO-K1 cells that associate with GPR139 to form a heterodimer. Whether such a complex formation is required for ligand interaction remains to be elucidated.

GPR139 and more so GPR142 were extremely inefficient in transient transfections. Even in stable cell lines GPR142 expression was much lower than that of GPR139. We found that the proteasome inhibitor MG-132 improved the stability and cell-surface expression of GPR142, as evidenced by western and FACS analyses. This suggests that proper folding may require a chaperone or more time. The missing cysteines in extracellular loops one and two, which are characteristic for GPCRs, and the extended amino-terminal domain of GPR142 may contribute to destabilisation of the receptor structure.

Expression studies revealed that GPR139 is present predominantly in the mouse brain, both in the adult and during development. In the embryonal brain GPR139 showed a much more widespread distribution than in the mature central nervous system, indicative of a function for the development of distinct brain areas. Northern-blot analyses further showed high mRNA levels in distinct areas of the human brain, including putamen, caudate nucleus, and medulla, confirming the in situ hybridisation results in the mouse obtained by us and others (Matsuo et al., 2005). GPR142 mRNA was detected with high intensity in several peripheral organs and tissues, but was also present in the adult and more so in the developing mouse brain. In contrast to GPR139, which seemed to be expressed in distinct areas of the brain and during specific stages of mouse-brain development, GPR142 was more ubiquitously expressed and showed a certain preference for tissues and cells of mesodermal origin. From this we conclude that GPR142 may play a role not only in brain, but also in bone and blood formations. The presence of GPR139 in brain areas involved in motor control suggests a function as mediator in locomotor activity. Identification of a ligand or of ligands for both receptors may help to clarify their function.

Acknowledgements

We thank J. Stables for kindly providing vectors containing apoaequorin and Gα16, A. Methner for the luciferase-reporter-gene constructs, A. Ignatov and M. Rezgaoui for critical comments on the manuscript and S. Hempel for help with the figures.

References

Bockaert, J., Pin, J.P., 1999. Molecular tinkering of G protein-coupled receptors: an evolutionary success. The EMBO Journal 18, 1723–1729.

Boels, K., Hermans-Borgmeyer, I., Schaller, H.C., 2004. Identification of a mouse orthologue of the G-protein-coupled receptor SALPR and its expression in adult mouse brain and during development. Brain Research Developmental Brain Research 152, 265–268.

Civelli, O., 2005. GPCR deorphanizations: the novel, the known and the unexpected transmitters. Trends in Pharmacological Sciences 26, 15–19.

Fitzgerald, L.R., Mannan, I.J., Dytko, G.M., Wu, H.-L., Nambi, P., 1999. Measurement of responses from Gi-, Gs-, or Gq-coupled receptors by a multiple response element/cAMP response element-directed reporter assay. Analytical Biochemistry 275, 54–61.

Foord, S.M., Bonner, T.I., Neubig, R.R., Rosser, E.M., Pin, J.-P., Davenport, A.P., Spedding, M., Harmar, A.J., 2005. International Union of Pharmacology. XLVI. G protein-coupled receptor list. Pharmacological Reviews 57, 279–288.

Frederiksson, R., Lagerström, M.C., Lundin, L.G., Schiöth, H.B., 2003a. The G-protein-coupled receptors in the human genome form five main families. Phylogenetic analysis, paralogon groups, and fingerprints. Molecular Pharmacology 63, 1256–1272.

Frederiksson, R., Höglund, P.J., Gloriam, D.E.I., Lagerström, M.C., Schiöth, H.B., 2003b. Seven evolutionarily conserved human rhodopsin G protein-coupled receptors lacking close relatives. FEBS Letters 554, 381–388.

Gloriam, D.E.I., Schiöth, H.B., Frederiksson, R., 2005. Nine new human rhodopsin family G-protein coupled receptors: identification, sequence characterisation and evolutionary relationship. Biochimica et Biophysica Acta 1722, 235–246.

Hökfelt, T., Bartfai, T., Bloom, F., 2003. Neuropeptides: opportunities for drug discovery. Lancet Neurology 2, 463–472.

Ignatov, A., Lintzel, J., Kreienkamp, H.J., Schaller, H.C., 2003a. Sphingosine-1-phosphate is a high-affinity ligand for the G protein-coupled receptor GPR6 from mouse and induces intracellular Ca^{2+} release by activating the sphingosine-kinase pathway. Biochemical and Biophysical Research Communications 311, 329–336.

Ignatov, A., Lintzel, J., Hermans-Borgmeyer, I., Kreienkamp, H.J., Joost, P., Thomsen, S., Methner, A., Schaller, H.C., 2003b. Role of the G-protein-coupled receptor GPR12 as high-affinity receptor for sphingosylphosphorylcholine and its expression and function in brain development. The Journal of Neuroscience: The OfficialJournal of the Society for Neuroscience 23, 907–914.

Jiang, C., Chen, G., Zeng, X., Quyang, K., Hu, Y., 2003. Generation of a bioactive neuropeptide in a cell-free system. Analytical Biochemistry 316, 34–40.

Joost, P., Methner, A., 2002. Phylogenetic analysis of 277 human G-protein-coupled receptors as a tool for the prediction of orphan receptor ligands. Genome Biology 3. research0063.1–0063.16.

Kayser, S.T., Ulrich, H., Schaller, H.C., 1998. Involvement of a Gardos-type potassium channel in head activator-induced mitosis of BON cells. European Journal of Cell Biology 76, 119–124.

Matsuo, A., Matsumoto, S.-I., Nagano, M., Masumoto, K.-H., Takasaki, J., Matsumoto, M., Kobori, M., Katoh, M., Shigeyoshi, Y., 2005. Molecular cloning and characterization of a novel Gq-coupled orphan receptor GPRg1 exclusively expressed in the central nervous system. Biochemical and Biophysical Research Communications 331, 363–369.

Stables, J., Green, A., Marshall, F., Fraser, N., Knight, E., Sautel, M., Milligan, G., Lee, M., Rees, S., 1997. A bioluminescent assay for agonist activity at potentially any G-protein-coupled receptor. Analytical Biochemistry 252, 115–126.

Süsens, U., Aguiluz, J.B., Evans, R.M., Borgmeyer, U., 1997. The germ cell nuclear factor mGCNF is expressed in the developing nervous system. Developmental Neuroscience 19, 410–420.